Model-based Voltage Prediction for a Zinc-Air Cell subject to Piecewise Constant Discharge Currents

Juan Diego Pineda Rodriguez, Sorin Olaru, Cristina Vlad, Pedro Rodriguez-Ayerbe, Woranunt Lao-Atiman, Soorathep Kheawhom

Model-based Voltage Prediction for a Zinc-Air Cell subject to Piecewise Constant Discharge Currents

Juan Diego Pineda Rodriguez[1], Sorin Olaru[1], Cristina Vlad[1], Pedro Rodriguez-Ayerbe[1], Woranunt Lao-atiman[2], Soorathep Kheawhom[2]

***Abstract*—The paper is dedicated to the modeling of the dynamical behavior of a Zinc-Air battery. The main goal is to construct a model-based prediction mechanism for the output voltage of the battery cell as a function of the discharge current profile. There are several difficulties behind this construction, mainly related to the nonlinear behavior, the high influence of the cell geometrical configuration, and ultimately the impact of the measurements in the transitory. The current work goes a step forward with respect to the constant current models developed in the previous studies and enhances a series of modeling hypotheses through the analysis of a piece-wise constant discharge profile.**

The important advantage of the results presented in the current work is related to the real-data measurements accompanied by the detailed pre-treatment procedures and, finally, to the construction of the model and the comparison with the existing alternative approaches.

***Index Terms*—Energy storage system; Dynamical model of batteries, Parameter identification.**

I. Introduction

The awareness of the global impact of human activity and the viability constraints nourishes the interest in safe and sustainable energy production-transmission-distribution. The importance of energy storage systems is growing [1] in this context. Firstly used for reducing power fluctuations, it evolved towards a control lever for the emergence and flexibility of electricity generated by renewable energy sources. Indeed, energy storage systems mitigate renewable energy variability whenever the production units are associated with them. For efficient functioning, the energy storage unit would ideally present a large capacity and fast response time [2].

In the quest for these systems, batteries have an important place due to the mobility and interoperability of their architecture. Estimation and control techniques are the key enablers in this respect [3]. There is an effort from fundamental research spanning from the chemistry of the batteries [4] to material sciences, which brings advances in effective construction [5] and control engineering, which provides stable and robust operation of novel configurations [6]. In this regard, and due to its availability, Zinc based batteries have attracted the research community's interest with Zinc-air as one of the most studied configurations.

[1]The first four authors are with Laboratory of Signals and Systems, Université Paris-Saclay, CNRS, CentraleSupélec, 91190 Gif-sur-Yvette, France {diego.pineda;sorin.olaru;cristina.vlad;pedro.rodriguez}@centralesupelec.fr

[2]The last two authors are with Department of Chemical Engineering, Faculty of Engineering, Chulalongkorn University, Bangkok 10330, Thailand {Woranunt.L;Soorathep.K}@chula.ac.th

The first studies were dedicated to the intrinsic properties of the materials and components [7], while the latest research on Zinc-airflow batteries concentrates on the operation [8], in particular through the construction of a battery management system able to use model-based approaches to optimize the functionality in real-time.

In the previous studies [9]- [10], the nonlinear characteristics are stressed regarding the transitory, and the modeling attempts have been exploiting Hammerstein-Wiener approaches or linear time-varying techniques. However, another battery feature must be identified to provide a good prediction capability: state-of-charge evolution or open-circuit voltage evolution in different approaches. The latter is the most sensitive parameter in battery modeling because it represents the essential indicator for depletion. The existing results on this topic [11] exploit curves obtained at different constant discharge currents up to the complete depletion. This approach is reliable for identifying the evolution of the output voltage but ignores the transitory effects. It thus relates the SoC (output-voltage) evolution to the current-counting process. Once the discharge curves are identified based on different constant current levels, interpolation is used to obtain a generic model for the SoC evolution along a potentially time-varying current profile.

The main criticism that can be addressed to this approach is that each constant-current curve is recorded for a different realization of the primary cell, meaning that Zinc granules, electrolyte, temperature, and other relevant context parameters are different between experiments. This variability can be understood as a random process and should be analyzed. Unfortunately, the number of experiments [12] doesn't allow a statistical treatment. Moreover, measurements exhibit non-monotonic behavior, which can further appear in an explicit form in the interpolation scheme.

The present paper aims to explore a different approach to identifying the open-circuit relationship between the discharge current and the output voltage by reducing the impact of the variability of the context parameters. The novel methodology exploits a piece-wise constant discharge profile and aims to obtain information on the discharge curves without creating a new cell. While the advantage is information-rich measurements, the procedure must face a particularly complex treatment of the transitories at the constant discharge current commutation. We will present in detail the proposed methodology and conclude with a model identification of the overall dependence of the output voltage on the current counting.

The approach is compared with the existing one in the literature. This analysis points to the impact of uncertainties in both strategies. Still, it has the advantage of comforting the monotonicity hypothesis for the model parameters as a function of the discharge current. This aspect was missing from the existing studies and is essential in the prediction-based battery management system design.

The paper is organized as follows: Section II recalls the principles of functioning for the Zinc-air battery under study and describes the particularities of the modeling problem. Section III presents the main steps of the new methodology along with the assumptions and tools employed. Section IV presents the results obtained from real-world measurements and analyzes the characteristics compared to the existing approaches.

II. System description

A. Cell functioning

Zinc-air batteries (ZAB) are energy storage devices that can accumulate and release energy due to an electrochemical reaction. These batteries use Zinc (Zn) and (O_2) as reactants, abundantly available in the atmosphere. The discharge process is based on a redox reaction: oxygen reduction and Zinc metal oxidation that produces zincate, which later leads to zinc oxide. The prototype of the zinc-air battery considered in the current study was developed by Chula University in Bangkok and consists of a Zn anode (negative) and an air cathode (positive).

A potassium hydroxide (KOH) solution with a concentration of $7M$ is used as an electrolyte. During discharge, Zn oxidation proceeds at the anode. Zn reacts with hydroxide ions (OH^-) to generate zincate ion ($Zn(OH)_4^{2-}$) and electrons. $Zn(OH)_4^{2-}$ is precipitated to zinc oxide (ZnO) when its concentration exceeds the saturation limit. The electrons generated from the anode are transferred to the cathode via the external circuit. At the cathode, O_2 from the atmosphere receives electrons and is converted to OH^-. The reactions at the anode and cathode are:

- Anode:

$$Zn + 4OH^- \longleftrightarrow ZnOH_4^{2-} + 2e^-$$

$$ZnOH_4^{2-} \longleftrightarrow ZnO + 2OH^- + H_2O$$

$$(E^0 = -1.25 \text{ V vs SHE})$$

- Cathode:

$$\frac{1}{2}O_2 + H_2O + 2e^- \longleftrightarrow 2OH^-$$

$$(E^0 = 0.401\text{V vs SHE})$$

The chain of reactions can be resumed at the level of the zinc-air battery in the following terms:

$$Zn + \frac{1}{2}O_2 \longleftrightarrow ZnO$$

$$(E^0_{\text{cell}} = 1.65V)$$

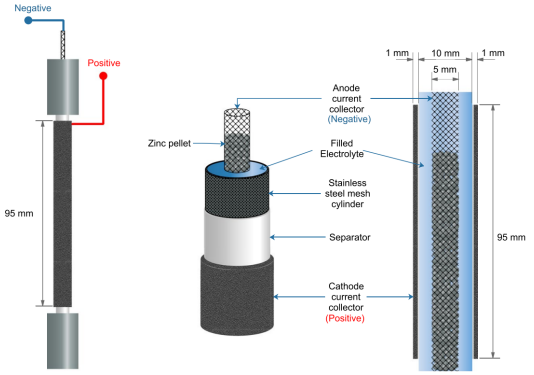

Fig. 1. The structure of the Zinc-air battery [12].

The theoretical equilibrium potential of the zinc-air battery is 1.65 V. The measured open circuit potential is around 1.4 V for the prototype in this study.

The device used for measurement was the Battery Test System BTS-4000 series from Neware; an 8-channel testing device connected to a server for data transmission. The latter is connected to a laptop through an Ethernet cable. The overall system allows programming the desired current/voltage profiles for battery charge/discharge testing; constant voltage, current, or power. The cell is primary in this study; it has to be changed after every discharge cycle and the device is then programmed to a constant current discharge. The sampling time for the tests is 100 ms, and the cut-off voltage is 0.01 V.

B. Basic principles of operation

The chemical reaction helps to understand the general principle of operation of the cell. Still, it does not provide an effective mechanism for predicting voltage and current dynamics with the available data, since electrochemical modeling would require knowledge of physical parameters on different spatio-temporal layers. As such information is unavailable, a grey box method is used to obtain a general model of the cell through measured data and expected dynamics based on observation. Available data consists of the desired current as an input and the cell's voltage as an output. Accordingly, the cell's *available* capacity (or State of Charge) can be inferred whenever the cell's voltage starts dropping for a given operating current.

A basic model can be established as shown in Fig. 2 where the integral of the input current $i(t)$ is the cell's *discharged capacity*, also known as *current-counting* measure C in amp-hours (Ah). We also remark the impact of the context variable in the output voltage (temperature, quality of the electrolyte, tube coating, etc.).

Once these elements are available, the system can be analyzed in two separate stages:

- The constant current discharge behavior, given by a nonlinear function $f(.)$, which describes the cell's voltage during its entire discharge period (usually in hours). This allows us to monitor the state of charge and identify the point of cell depletion.

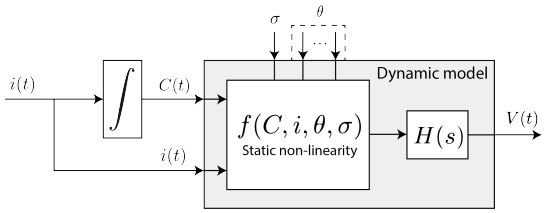

Fig. 2. Block diagram describing the system.

- A dynamical behavior (fast variation), which describes the cell's change in voltage as a response to a change in current, given by the transfer function $H(.)$.

Since the cell is changed after every discharge, a context parameter vector θ impacts the function $f(.)$ to include the variations from cell to cell, such as Zinc quantity inside the tube, temperature, electrolyte quality, etc. These parameter changes will affect the cell's open-circuit voltage and available capacity. The parameter in itself can be considered as a random variable. Aging phenomena is a different and independent parameter that will be denoted as σ in the block diagram. It affects the cell's performance after several tests (which degrade the coating). There exists an explicit dependence of the static nonlinearity $f(.)$ in θ and σ.

This study focuses on finding a suitable function $f(.)$ to predict the discharge characteristics of the cell. From the behavior of different discharge profiles, one can extract some basic principles of operation that we aim to retrieve in the modeling process:

- Monotonic decrease of the output voltage with the increase of the discharge current; $V(C, i_1) > V(C, i_2), \forall\ |i_1| < |i_2|$.
- Along with the evolution of the *used capacity*, the output voltage decreases; $V(C_1, i) > V(C_2, i), \forall\ C_1 < C_2$.

C. Modeling

Battery modeling is a key step towards effective operation and integration in any application [13]. For a novel architecture like Zinc-air, the modeling phase can build on the similarities with the alternative technologies (e.g. Li-Ion) but should also capture the particularities. Zinc-air cell voltage characteristics differ from other constructions mainly in the high variability of its magnitude in response to demanded currents; other chemistries tend to maintain a fairly constant voltage for different currents, which is not the case for Zinc-air. However, the discharge curve's shape remains similar to other types of cells. In consequence, a sigmoidal structure can be selected to describe the cell's discharge, with important parameters:

1) Sigmoid's maximum, noted as A, in this case corresponds to the cell's maximum steady-state output voltage. This voltage varies monotonically as a function of the current.
2) Sigmoid's midpoint or inflection point, noted as C_{in}, is a function of the cell's used capacity and current, which tells when the cell has reached depletion and cannot deliver the setpoint current anymore.
3) Sigmoid's slope at the inflection point, noted as C_1, is a function of the current.

The model in [11] is one of the methods that can be adopted to find an appropriate cell model. It proposes two sigmoidal structures to describe the cell's voltage characteristics (Boltzmann and bi-phasic). There are no transitory effects, so the block diagram can be reduced to the diagram in Fig. 3. In the current work, we preserve the principle but propose a slightly different (simplified) sigmoid function for the voltage approximation, where the voltage of the cell is given as a function of the current i and the cell used capacity C (measured in Ah):

$$V(C, i) = \frac{A(i)}{1 + \mathrm{e}^{C_1(i)(C - C_{in}(i))}} \tag{1}$$

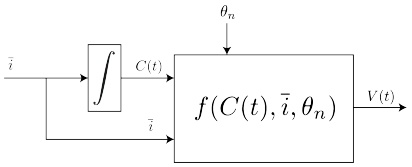

Fig. 3. Block diagram for a constant current $\bar{i}$, including the construction parameter uncertainty.

The construction parameter uncertainty θ is added to the diagram, and σ is not considered as the aging between tests can be neglected (the tests are performed in a small period separating them). Here, θ_n is the parameter represented by a discrete random variable corresponding to one particular test on a cell. This method allows analysis for complete discharges. However, due to the high variability between cells (e.g. open-circuit voltages), it is necessary to have an extensive test database to create a statistical model that fits the system. This variation between $\theta_n \rightarrow \theta_{n+1}$ modifies the tendencies of C_1, C_{in}, and A, as seen in Fig. 4a and Fig. 4b where these parameters show not fulfilling the monotonicity hypothesis. Also, multiple testing of the cell degrades it over time and approaches it to the end of its life. This results in higher variability of θ between tests and even affects its performance (open-circuit voltage, the current it can deliver, and available capacity), hindering the possibility of correctly establishing a global model.

The subsequent developments aim to identify the dependence of the parameters C_1, C_{in}, and A to establish a cell discharge model. Transient response for changes in current is not considered in this paper (we refer to [9]- [10] for addressing it). To be able to do this, it is necessary to establish a correct test protocol to minimize the effects of parameter uncertainty (θ) on the global model.

III. A NOVEL APPROACH FOR PARAMETER IDENTIFICATION

To overcome the difficulty of imposing the monotonicity in modeling and cell aging, multiple current profiles within the same discharge cycle can be used to minimize the impact of cell-to-cell variability and confirm or invalidate the

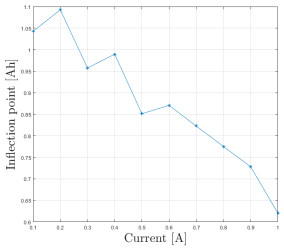

(a) Inflection points vs Current

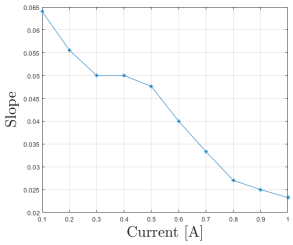

(b) Sigmoid's slope vs Current.

Fig. 4. Previous study inflection points and sigmoid's slope.

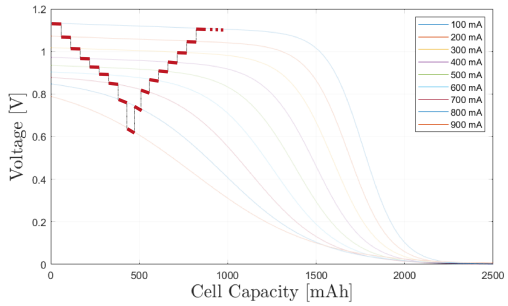

Fig. 6. Partial data sigmoid reconstruction.

monotonicity hypothesis. In such a modeling framework, the block diagram in Fig. 2, there is a unique, constant $\bar{\theta}$. The function $f(.)$ depends exclusively on the capacity[1] and the current. Parameter σ is no longer taken into account.

A. Data treatment

Multiple current steps within the same discharge cycle are considered to avoid the variability of cell-to-cell construction parameters; a regular increase/decrease ranging from 100 mA to 900 mA, in 100 mA variations as shown in Fig. 5. This profile was repeated until reaching the cell's depletion. The discharge monitoring process is supervised. Whenever the battery is depleted and cannot deliver the current set-point, the respective value is abandoned, and the reference current is modified to the next in the sequence. This allows the selection of the best feasible discharge current in the periodic sequence.

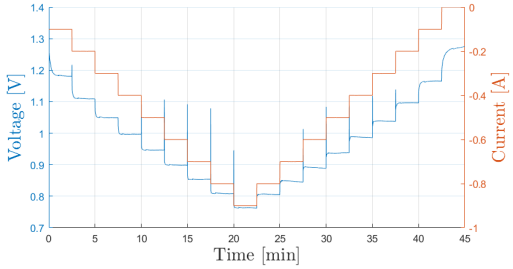

Fig. 5. Cell voltage obtained for the considered current profile.

As a novelty, we exploit the fact that a sigmoid can be reconstructed using the steady-state values of the voltage for a piecewise constant discharge current, as illustrated conceptually in Fig. 6. The red curves represent the voltage fragments superimposed on the sigmoid behavior the entire fragment group is expected to follow at different constant currents. Several such fragments obtained along the discharge cycle allow the reconstruction of a sigmoid. Actual test fragments following this trend are shown in Fig. 9, 10, and 11.

Based on this principle, to obtain fragments of voltage measurement for every test current, the data portrayed in Fig. 5 has been split according to each current. Since the objective here is to study the steady-state behavior of the cell, data had to be treated to eliminate the transient behavior when there is a step change in the current discharge profile. This was done by analyzing the time constant for each step current to retain the steady values. Eliminating the samples on the transitory also eliminates the voltage peaks at the beginning of each current step seen in Fig. 5. Treated data is presented in Fig. 7. This new fragmented data facilitates its analysis to obtain a global constant discharge model. There are two criteria for storing a data fragment:

- Intervals longer than 30 seconds and shorter or equal to 2.5 minutes (the current step size) are kept with their steady-state voltage. The first 30 seconds from each fragment are cut since a preliminary time constant τ was identified as 6.7 s, so $5\tau \approx 33$ s.
- Fragments shorter than 30 seconds are not taken into account since the set-point current is not delivered. The fragment is, therefore, not relevant to account for the tendency.

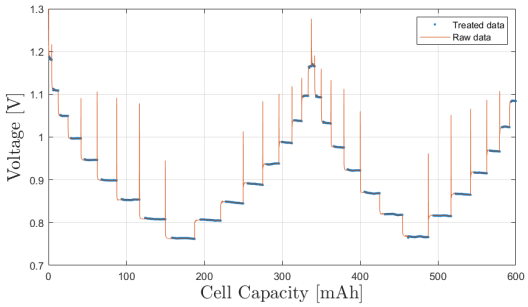

Fig. 7. Output voltage fragments after data treatment.

B. Model fitting

Once the data is trimmed and the steady-state voltage is retained, the model fitting can be employed. Nonlinear least squares algorithm is applied to identify each parameter on (1), starting from first-order polynomials for A, C_{in}, and C_1, and adding complexity to fit the model better, based on RMSE and R^2 values for each iteration.

The results obtained for (1) with parameters as first-order polynomials provide a poor fit for the data measured during

[1]In the sequel, the cell's **used** (or discharged) capacity will be referred to as "Capacity".

the tests. It is thus necessary to move to nonlinear analysis, particularly concerning the inflection point and the sigmoid's maximum, where a dependence on the cell's capacity is considered. In addition, the intervals after the first visible drop-point are eliminated from data fitting as the cell enters a nonlinear transitory behavior when approaching the end of discharge. The retained expressions are:

$$A(i) = \zeta i^2 + \gamma i + \delta + \eta C \tag{2}$$

$$C_1(i) = \beta i + \alpha \tag{3}$$

$$C_{in}(i) = \varepsilon \mathrm{e}^{-i} - \rho \tag{4}$$

IV. Model Validation and Comparative Analysis

Based on the expressions (2), (3), and (4), the fitted coefficients are provided in Table I.

TABLE I
COEFFICIENT VALUES FOR SURFACE FITTING

Parameter	Coefficient	Value
A	ζ	0.396
	γ	0.735
	δ	1.203
	η	$-2.893\text{x}10^{-5}$
C_1	β	$8.49\text{x}10^{-3}$
	α	0.01
C_{in}	ε	-700
	ρ	-2541

The surface obtained for this set of coefficients, portrayed in Fig. 8, outperforms the curves obtained for simpler polynomials; the RMS error for the final surface has a value of 0.024, lower than previous models, and the determination coefficient R^2, went from low values to 0.96. It is possible to observe that the sigmoid slope at the drop point is steeper for lower currents, as observed in previous and present studies, and that the maximum voltage decreases as expected for increasing currents due to the cell's internal equivalent series resistance.

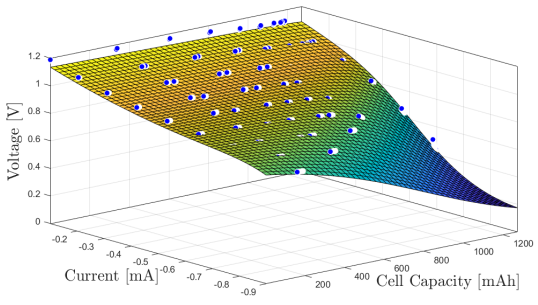

Fig. 8. Fitted surface to final coefficients.

To validate the resulting model, three steps were followed:

1) A curve for each current was obtained using the model and compared to the actual data, as observed in Fig. 9.
2) The original, pyramid-like input was then applied to the model, obtaining the curves depicted in Fig. 10. A very good fit is expected as this input is used to identify the model parameters.
3) Finally, a different current profile was applied to the cell and the experimental data is compared to the model output, shown in Fig. 11. This will be the validation data set.

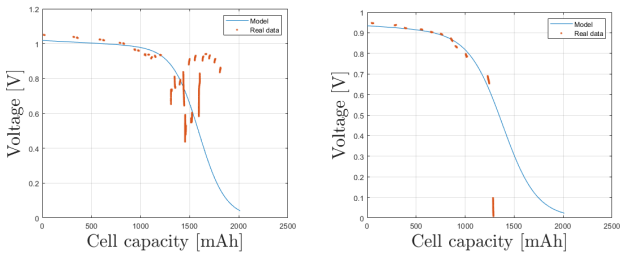

(a) $i = 300$ mA (b) $i = 500$ mA

Fig. 9. Comparison of output voltage obtained with the model to real data.

As can be noted in the fitted surface and in the comparisons with the real data, the model fits less for large amplitude currents, which can result from fewer data fragments for large amplitude currents. It is important to mention as well that, when approaching the end of the discharge, the steady voltage for one current is affected by the voltage of a larger preceding current, as the stabilization time is often longer, and it may not reach a steady state before a next current step change. This result affects the global curve, as seen in Fig. 9a.

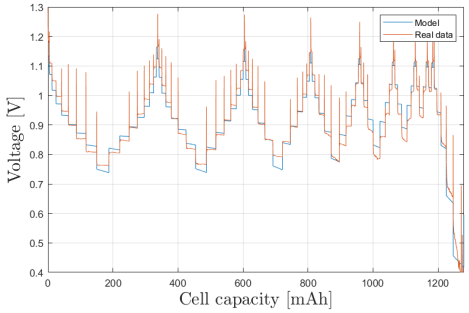

Fig. 10. Comparison of the model output to the estimation data profile.

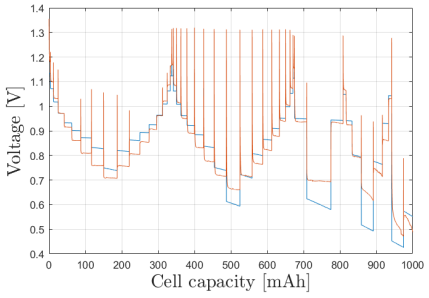

Fig. 11. Comparison of the model output to the validation data profile.

In addition, a comparison of the sigmoid parameters as a

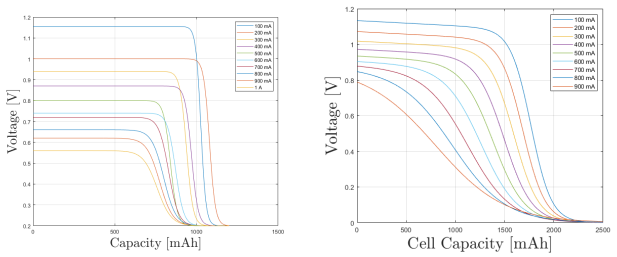

(a) Voltage curves obtained from the model in previous studies.

(b) Voltage curves from the present study.

Fig. 12. Comparison of voltage curves obtained in previous studies and the ones obtained with the present model

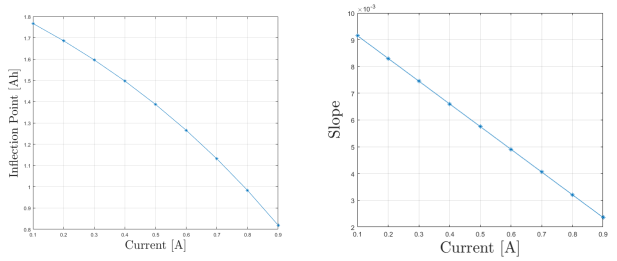

(a) Inflection points.

(b) Sigmoid slopes.

Fig. 13. Inflection points and slopes for the present study.

function of the current was also made to verify the monotonicity hypothesis. Here, the parameter tendencies are compared to the ones obtained in [11], which are based on constant current discharge. Starting with the inflection points, one can notice the superposition of the curves in Fig. 12a, which proves non-monotonicity in the previous study due to the variability in the cell operation. This can be seen more clearly when comparing with Fig. 4a. New inflection points in Fig. 13a confirm monotonicity.

Similarly, comparing the sigmoid's slopes in Fig. 4b to the ones in Fig. 13b, the monotonicity assumption can be verified in the present study from the resulting identified model. Finally, as an additional validation of the proposed model in comparison with the one in [11], the current profile from the validation set of Fig. 11 was applied to both models, resulting in an RMS error of 0.261 for the old model and of 0.0683 for the model developed in this study, confirming the interest of the present approach.

Based on these observations, the approach used for obtaining the model allows one to overcome the construction parameter uncertainty θ, so it is possible to demonstrate and assure monotonicity in the voltage response of the cell. However, even if the sensibility to θ is avoided, the presented procedure faces a new source of uncertainty: the transient states at the transition between piecewise constant discharge currents.

V. Conclusion

The present work on modeling Zinc-air batteries started from the fact that constant current discharge exhibits a high variability concerning the realization of cells. This variability made the validation of the monotonicity assumptions for the parameters of the sigmoid-like models impossible. Two main contributions based on real-time measurements and associated treatment of the data emerge from the current study. On one side, the piecewise constant discharge currents can provide insightful information for the parameter identification procedure using a single cell. On the other side, all the parameters of the sigmoid function exhibit a monotone dependence on the discharge current. The fitting process is highly impacted by the transitory effects at the switch between different discharge current levels. The present work provides preliminary validation in this respect, and further systematic procedures must be developed to perform the parametric identification automatically.

On a broader scope, the variability was mitigated from the parameter identification at the level of a cell but its impact cannot be ignored in the transition from one cell functioning to the other. In this respect, an adaptive procedure for adjusting parameters should be investigated to allow the embedding in a Battery Management System.

References

[1] V. A. Boicea, "Energy storage technologies: The past and the present," *Proceedings of the IEEE*, vol. 102, no. 11, pp. 1777–1794, 2014.

[2] S. O. Amrouche, D. Rekioua, T. Rekioua, and S. Bacha, "Overview of energy storage in renewable energy systems," *International journal of hydrogen energy*, vol. 41, no. 45, pp. 20 914–20 927, 2016.

[3] S. J. Moura, "Estimation and control of battery electrochemistry models: A tutorial." in *CDC*. Citeseer, 2015, pp. 3906–3912.

[4] S. Suren and S. Kheawhom, "Development of a high energy density flexible zinc-air battery," *Journal of the Electrochemical Society*, vol. 163, no. 6, p. A846, 2016.

[5] V. Sulzer, P. Mohtat, A. Aitio, S. Lee, Y. T. Yeh, F. Steinbacher, M. U. Khan, J. W. Lee, J. B. Siegel, A. G. Stefanopoulou *et al.*, "The challenge and opportunity of battery lifetime prediction from field data," *Joule*, vol. 5, no. 8, pp. 1934–1955, 2021.

[6] A. Abbasi, S. Hosseini, A. Somwangthanaroj, R. Cheacharoen, S. Olaru, and S. Kheawhom, "Discharge profile of a zinc-air flow battery at various electrolyte flow rates and discharge currents," *Scientific data*, vol. 7, no. 1, pp. 1–8, 2020.

[7] W. Lao-Atiman, K. Bumroongsil, A. Arpornwichanop, P. Bumroongsakulsawat, S. Olaru, and S. Kheawhom, "Model-based analysis of an integrated zinc-air flow battery/zinc electrolyzer system," *Frontiers in Energy Research*, vol. 7, p. 15, 2019.

[8] W. Lao-atiman, S. Olaru, and S. Kheawhom, "Linear parameter-varying model for prediction of charge/discharge behavior of tri-electrode zinc-air flow battery," *IFAC-PapersOnLine*, vol. 55, no. 16, pp. 92–97, 2022.

[9] W. Lao-atiman, S. Kheawhom, and S. Olaru, "Zinc-air battery dynamics' identification using transfer functions and hammerstein-wiener models," in *2019 23rd International Conference on System Theory, Control and Computing (ICSTCC)*. IEEE, 2019, pp. 332–337.

[10] W. Lao-Atiman, S. Olaru, S. Diop, S. Skogestad, A. Arpornwichanop, R. Cheacharoen, and S. Kheawhom, "Linear parameter-varying model for a refuellable zinc–air battery," *Royal Society open science*, vol. 7, no. 12, p. 201107, 2020.

[11] S. Olaru, A. Golovkina, W. Lao-atiman, and S. Kheawhom, "A mathematical model for dynamic operation of zinc-air battery cells," *IFAC-PapersOnLine*, vol. 52, no. 17, pp. 66–71, 2019.

[12] W. Lao-Atiman, S. Olaru, A. Arpornwichanop, and S. Kheawhom, "Discharge performance and dynamic behavior of refuellable zinc-air battery," *Scientific data*, vol. 6, no. 1, pp. 1–7, 2019.

[13] G. L. Plett, *Battery management systems, Volume I: Battery modeling*. Artech House, 2015.